Fuel 164 (2016) 339–346

Contents lists available at ScienceDirect

Fuel

journal homepage: www.elsevier.com/locate/fuel

Catalytic synthesis of mixed alcohols mediated with nano-MoS_2 microemulsions

Julia K. Hasty [a], Sathish Ponnurangam [b], Scott Turn [c], P. Somasundaran [b], Taejin Kim [a], Devinder Mahajan [a,d,*]

[a] Department of Materials Science and Engineering, Stony Brook University, Stony Brook, NY 11794, USA
[b] Department of Earth and Environmental Engineering, Columbia University, New York, NY 10027, USA
[c] Hawaii Natural Energy Institute, University of Hawaii, Honolulu, HI 96822, USA
[d] Sustainable Energy Technologies Department, Brookhaven National Laboratory, Upton, NY 11973, USA

ARTICLE INFO

Article history:
Received 25 February 2015
Received in revised form 14 September 2015
Accepted 16 September 2015
Available online 2 October 2015

Keywords:
Syngas
Mixed alcohols
MoS_2
Nanoparticles
Microemulsion

ABSTRACT

Supported micron-sized molybdenum disulfide (MoS_2) has been extensively studied for catalytic synthesis of Higher Alcohols Synthesis (HAS) from synthesis gas (syngas). However, the process is associated with low space–time–yield (STY) and poor selectivity under high temperature (300–325 °C) and high pressure (10–20 MPa) operation, making it unattractive for commercial application. Nano-sized MoS_2 catalyst particles improve selectivity to alcohols but the yields are low possibly due to catalyst aggregation and mass transfer limitations. This study describes the use of oil-in-polyethylene glycol (PEG) microemulsion-based encapsulation of hydrophobic catalyst nanoparticles (MoS_2) to prevent aggregation, increase surface area and increase mass transfer across the two phases. In this study, nano-sized MoS_2 was first synthesized by sonolysis of hexacarbonyl molybdenum and yellow sulfur in hexadecane in <90% yield, mixed with non-ionic surfactant (Tergitol NP-8) and the mixture was slurried in two solvents: PEG-400 or Ethylflo-164 (a C30 oil). The slurred nano MoS_2 was evaluated for syngas (H_2/CO = 2:1) conversion into higher alcohols in a 300 mL stirred batch reactor. Our results showed increased STY, reaching 1.2 kg alcohols/kg catalyst/h. The corresponding product selectivity reached 62 wt% methanol and 52 wt% to ethanol, respectively in two separate runs when microemulsion-based catalysts were employed. These results open up the possibility of a novel and efficient route to higher alcohols.

1. Introduction

The use of fossil fuels is considered largely responsible for measured increase in the atmospheric CO_2 levels (36% since 1800s [1]), causing a 1.4 °F rise in the earths average temperature (from 1900 to 2000 [2]) and an increase in ocean acidity of 30% since the industrial revolution. Advancements in efficient biofuel technologies from sustainable and waste biomass are important for replacing fossil fuel demand, mitigating climate change, and addressing national security concerns. The Department of Energys Billion-Ton Study by Oak Ridge National Laboratory estimates a projected availability of up to 1.6 billion tons of sustainable biomass for processing by 2030 [3]. The process investigated in this paper is the thermo-chemical pathway involving two distinct steps: (1) thermal decomposition (gasification) of biomass to synthesis gas followed by: (2) catalytic conversion of synthesis gas into higher alcohols. The advantages of this route include the co-production of heat and/or electricity from the exothermic catalytic reaction during the Higher Alcohols Synthesis (HAS) process.

Molybdenum disulfide (MoS_2) remains the most studied catalyst for the production of higher alcohols from synthesis gas [4,5], though technological hurdles including high operating pressures, low product yields and selectivity remain to consider this system commercially viable. A series of alkali-doped MoS_2 based catalysts were first patented by Dow Chemicals (now Union Carbide) in the 1970s. There is interest in these Mo-based catalysts for their ability to tolerate sulfur as wells as CO_2 in the reactant syngas stream while non-Mo catalysts are sensitive to sulfur at very low concentrations. The inherent tolerance to sulfur could potentially eliminate a need for the desulfurization step, thus decreasing the process cost. Typically, sulfided catalysts require 50–100 ppm sulfur in the gas stream to remain active. Also, MoS_2 displays high water–gas–shift (WGS) activity and demonstrates

* Corresponding author at: Department of Materials Science and Engineering, Stony Brook University, Stony Brook, NY 11794, USA. Tel.: +1 631 632 1813; fax: +1 631 632 6823.
E-mail address: devinder.mahajan@stonybrook.edu (D. Mahajan).

http://dx.doi.org/10.1016/j.fuel.2015.09.039
0016-2361/

higher selectivity toward ethanol than most other catalysts [6]. The operating temperature and pressure ranges of the sulfided Mo catalyst are 260–350 °C and 435–2540 psi respectively. The addition of sulfide enables the catalyst to promote hydrogenation. Similar to that of modified Fischer–Tropsch (F–T) catalysts, the modified sulfide catalysts follow the Anderson-Shultz Floury (ASF) product distribution [4]. The addition of an alkali directs products to alcohols instead of hydrocarbons by suppressing the tendency for the Mo active sites to promote hydrogenation [7,8]. Work has shown that the most effective alkali promoter is cesium, however potassium is commonly used [9]. A recent study showed that alkali- and metal-doped MoS_2 catalysts (M-K/MoS_2, M = Fe, Ni, Co) produced alcohols with a volumetric space–time–yield (STY) of 0.4 g/ml cat. h alcohols under operating conditions of 340 °C, 1378 psi, H_2/CO ratio of 1, and gas hourly space velocity (GHSV) of 8500 h^{-1} over 2000 h with no apparent decrease in both the catalyst activity and the alcohol selectivity [6].

While catalyst nanoparticles could potentially show significant improvement in productivity, there are still limitations to the reaction system. The slurry-phase MoS_2-catalyzed process is challenged with mass and heat transfer limitations in the presence of four phases (catalyst/non-aqueous/aqueous/gas). Thus, even with nano-sized catalysts, low yields are expected due to aggregation in a multi-phase environment. Thus, maximizing contact between various phases would increase STY. These challenges can be addressed by using supercritical solvents. A supercritical solvent can provide enhanced gas–liquid mass transfer due to unlimited CO_2 solubility in supercritical phase, higher diffusion rates, increased reaction rates due to higher solubility of products and prevention of catalyst poisoning as well as improved reaction selectivity [10]. The solvents in supercritical conditions such as carbon-dioxide (sc-CO_2), water (sc-H_2O) and hydrocarbons has already been used in several homogeneous and heterogeneous catalytic reactions [10–12].

Some examples of reactions that use sc-CO_2 as solvent and/or reactant include: (1) hydrogenation of olefinic oils [13,14], unsaturated ketones [15] and alcohols [16,17], (2) oxidation of alcohols [18] and hydrocarbons [19], (3) C–C bond formation [20–23] (4) hydroformylation [24–27] and (5) synthesis of formic acid and derivatives [28,29]. Supercritical hydrocarbons have been used in Fischer–Tropsch (F–T), methanol and higher alcohols synthesis [30–38]. These reactions were reported to have increased conversion rates as well as improved selectivity when operating under the supercritical phase. For reactants, catalyst and products that have widely differing polarity and low miscibility, phase transfer catalysis (PTC) offers an efficient process by which faster reaction rates and increased selectivity can be achieved [39–41]. A phase transfer catalyst with surface active properties (e.g., alkyl quaternary salts) can be used to extract hydrophilic reactants from the water phase and deliver it to organic phase [40]. Moreover, interaction of reactants with phase transfer catalyst can itself reduce the kinetic activation energy of the reactants. Using this approach, reaction rates were found to increase up to three orders of magnitude compared to single phase reactions [40]. PTC is used in biomass conversion, oxidation, alkylation, and hydrofluorination reaction to enhance catalytic activity [42–48]. Interestingly, a homogeneous pseudo two-phase solvent (micelle-, microemulsion-, or emulsion-based) for heterogeneous catalytic reactions combines advantages of the phase-transfer catalysis and supercritical solvent systems. In addition, this pseudo 2-phase system can potentially increase the exposed surface area of MoS_2 particles by containing them within microemulsion droplets that act as nano-reactors and thereby increase STY. Syngas components (CO, H_2 and CO_2), of interest here, have poor solubility in hydrophilic phases such as water or polyethylene glycol (PEG).

Though the micellization phenomenon in PEG liquid is not well studied, the ethoxylated surfactants such as pluronics and polysorbates are known for micellar and oil/PEG microemulsions, respectively [49,50]. One such family of ethyoxylated surfactants, nonylphenol ethyoxlate, has been extensively studied for preparing sc-CO_2 microemulsions in water [51,52]. Nanometer-sized MoS_2 encapsulated in microemulsion droplets under supercritical conditions (high temperature and pressure) would increase contact between reactants and intermediates with surfaces of MoS_2 catalyst particles. MoS_2 is well known for its high selectivity to C_2 alcohols and shows high stability with impurities, such as sulfur, in the feed gas stream [53].

Thus, our approach to improve heterogeneous catalytic higher alcohol synthesis (HAS) involves: (1) nano-sizing the traditional MoS_2 catalyst and (2) employing microemulsion medium to disperse MoS_2 nano-catalysts and increase contact with reactants. The premise is that a combination of the two would improve STY and selectivity for higher alcohols. This improvement would increase the economic feasibility of the technology to be an attractive candidate in the production of transportation fuels thus contributing to the Department of Energy renewable fuel standard (RFS) of 15 billion gallons [54].

2. Experimental

2.1. Reagents

The reagents were purchased from the following manufacturers: $Mo(CO)_6$ (Acros Organics), sulfur, anhydrous hexadecane, hexane and methanol (Sigma–Aldrich). Ethylflo-164 polyalphaolefin (a C-30 oil), Polyethylene glycol (PEG)-400 (Fluka Analytical), Commercial MoS_2 catalyst (<2 μm) (The Chemical Co.), Tergitol NP-8 (Dow Chemical).

2.2. Catalyst synthesis

Synthesis of nano-sized MoS_2 was achieved as follows. $Mo(CO)_6$ (0.02 mol) and elemental sulfur (S8) (0.02 mol) were slurried in 70 mL hexadecane solvent and added to a 300 mL sonication flask. The system was purged with argon before sonication to remove oxygen from the system. The sonicator (Misonix Sonicator 3000; 60 W) was programmed to pulse for 4 s followed by 1 s off time. The desired 70 °C temperature of the reaction vessel was maintained by placing the reaction vessel in a water-cooled bath. To monitor the extent of reaction, the evolved CO was collected in an inverted graduated cylinder from which the extent of $Mo(CO)_6$ decomposition was calculated at any given time. After about 30 h when the $Mo(CO)_6$ decomposition reached <90%, the sonication was stopped. The black slurry product was centrifuged, washed with n-hexane to yield a black powder. A detailed procedure developed by our group is described elsewhere [55,56].

2.3. Catalytic reaction

The batch evaluation of HAS reaction was conducted in a 300 mL Parr stirred pressure vessel fitted with a Parr process controller. For all runs, the slurry was pre-pared with 70 mL of either PEG-400 or C-30 oil solvent, 0.7 g of MoS_2 catalyst and specific amount (0.05 M, 0.01 M, and 0.002 M) of Tergitol NP-8 surfactant for batch evaluation. The above specified concentrations of Tergitol NP-8 surfactant were selected to ensure that the values were above the critical micellar concentration (CMC) in water (0.088–0.1 mM). The surface tension was measured using a surface tensiometer, Attension™ from Biolin Scientific employing the Wilhelmy plate technique. The slurry was then agitated using a homogenizer

(Power Gen 125, Fischer Scientific). The pressure vessel was purged with syngas and then pressurized to 600 psi syngas of composition 66% H_2/33% CO. Since the surfactant concentrations used was well above the CMC at the pressure, the formation of sc-CO-in-PEG microemulsions is expected. The pressure vessel was heated to an operating temperature of 250 °C, 270 °C, or 300 °C and an operating pressure between 800 and 900 psi. The reaction was allowed to run for approximately 8 h, quenched to room temperature and the final pressure was noted. Gas and liquid samples were then taken for analysis and subsequent mass balance as completed for each run. The completed batch runs are listed in Table 1. After the reaction, the catalyst particles were separated from the reaction slurry by centrifuge, washed with methanol, and dried at 70 °C for one hour to prepare for post-reaction analysis by transmission electron microscopy (TEM).

2.4. Analysis

A Perkin Elmer Frontier FT-IR spectrometer (380–4000 cm^{-1}) was used to map the vibrational spectra of the sonicated MoS_2 particles. The SEM images were obtained with SEM, LEO 1550 SFEG Microscope operated at a voltage of 15 kV. TEM (AMT Camera System; HV = 80.0 kV) was used to analyze surface topographies and particle size. For the analysis of reaction products, two GowMac 580 gas chromatographs (GCs) were configured to analyze gas samples from the batch runs. A Carboxen 1000 (45/60, 5′ × 1/8″) packed column was used for CH_4 and CO_2 analysis and a molecular sieve (9′ × 1/8″) packed column for CO analysis. For the CH_4, CO_2, and CO analysis, a He carrier was used (20 cc/min) using the following settings: column temperature, 60 °C; injector temperature, 60 °C; detector temperature, 90 °C; detector current, 150 mV. The injector sample used for both of these methods was 500 μL. The second GowMac 580 was set up for H_2 analysis (sample size 250 μL) using a molecular sieve 5A 80/100, 8′ × 1/4″) packed column with flowing N_2 carrier gas (18 cc/min) using the following settings: column temperature, 40 °C; detector temperature, 60 °C; detector current, 150 mV. A GowMac series 600 GC fitted with a thermal conductivity detector (TCD) and a Poropak Q (100/120, 9′ × 1/8″) packed column was used for the analysis of alcohols by injecting a 1 μL sample. The GC was first set up as follows: injector temperature, 200 °C; detector temperature, 250 °C and He as carrier gas (8 cc/min). Gas and liquid hydrocarbon samples were analyzed on a Perkin Elmer Clarus 680 GC fitted with an alumina (8′ × 1/8″) packed column with flowing He as carrier gas (20 cc/min). For analysis, an initial oven temperature of 120 °C held for 3 min; ramp of 30 °C/min to 250 °C. The sample size was 500 μL for gas analysis and 2 μ for liquid analysis.

3. Results and discussion

3.1. Catalyst synthesis

For catalyst synthesis using sonolysis, the initial off-white slurry consisting of $Mo(CO)_6$ (white powder) and sulfur (pale yellow powder) started to change color at the onset of sonication, and fully turned black within 10 min. During sonication, CO evolved that was carefully collected. The collected CO produced from $Mo(CO)_6$ decomposition was a measure of the extent of the reaction that indirectly measured disulfide molybdenum (MoS_2) formation following the stoichiometry Mo/CO = 1/6. The reaction was terminated by stopping sonication when the decomposition reached above 90%. A plot of CO evolution versus time (Fig. 1) shows that the observed $Mo(CO)_6$ decomposition analyzed for first-order kinetics with a rate constant $k = 3 \times 10^{-3}$ min^{-1} which is consistent with the value reported previously [55,56]. The FT-IR spectrum of the black product (Fig. 2) showed absorbance peaks indicative of as Mo–S (480 cm^{-1}) [57] and valence vibrations of Mo = S bond at 447 cm^{-1} and 453 cm^{-1} which is consistent with previous work [58].

Fig. 3 shows the scanning electron microscopy (SEM) image of MoS_2 as synthesized and after mixing with 0.01 M Tergitol NP-8 in PEG-400 at 270 °C. The figure shows spherical clusters and homogeneous size distribution with an average 15 nm size with the freshly synthesized MoS_2 sample (Fig. 3a). After mixing with the surfactant, however, the MoS_2 nanoparticles aggregate into larger size of over 200 nm (Fig. 3b). MoS_2 nanoparticles (Fig. 3a) are hydrophobic and hence can be expected to aggregate strongly since the samples were prepared by drying from a hydrophilic solvent, namely PEG-400. The TEM images of the synthesized MoS_2 particles, are shown in Fig. 4a and b for the catalyst with freshly prepared and after encapsulation with Tergitol NP-8, respectively. Fig. 4a shows that the particle sizes of fresh catalyst are 10–20 nm. After encapsulation, however, the material shows aggregated clusters, similar to those seen in the SEM images in Fig. 3 and consistent with previously reported work [55,56].

3.2. Batch evaluation of nano-MoS_2 catalyzed HAS reaction

The synthesized nanoparticles of MoS_2 were evaluated for syngas conversion into higher alcohols in a 300 mL Parr batch reactor. Eqs. (1) and (2) show the stoichiometries involved in CO hydrogenation to hydrocarbons and alcohols.

$$nCO + 2nH_2 \rightarrow (-CH_2-)_n + nH_2O \quad (1)$$

$$nCO + 2nH_2 \rightarrow C_nH_{2n+1}OH + (n-1)H_2 \quad (2)$$

$$H_2O + CO \rightarrow H_2 + CO_2 \quad (3)$$

Inevitably, CO_2 is also produced via the WGS reaction (Eq. (3)) under typical reaction conditions. Given that Eq. (3) accompanies alcohols synthesis, the syngas conversion ratio is established by the extent of Eq. (3), irrespective of the initial CO/H_2 ratio used. While the maximum stoichiometric ratio of H_2/CO is 2/1, due to the WGS reaction, theoretically the stoichiometric maximum is calculated to be 1.7 [59]. In this study a 66%/34% CO/H_2 ratio was used. The overall carbon conversion, carbon conversion (CO_2-free basis), STY and selectivity of the commercial and sonicated MoS_2 particles were measured and compared to previously reported

Table 1
Completed batch runs and corresponding operating conditions.

Run	B09	B10	B12	B13	B14	B15	B17	B82	B23	NP24	NP26
Catalyst	C	C	C	C	N	N	N	N	N	N	N
Solvent	PEG-400	PEG-400	C-30 Oil	C-30 Oil	C-30 Oil	PEG-400	PEG-400	PEG-400	PEG-400	PEG-400	PEG-400
Tergitol NP-8 (M)	0	0.040	0	0.049	0	0.051	0.049	0.053	0.002	0.011	0.030
Operating Temp. (°C)	300	300	300	300	300	300	250	270	270	270	270
C-Conversion (%)	28.7	16.7	32.2	12.9	41.4	91.2	21.8	51.7	48.0	50.5	42.2
C-Conversion (CO_2-free basis) (%)	18.3	6.2	32.0	12.7	29.8	36.6	14.7	33.4	27.5	28.6	16.9
STY Alcohols (mmol OH/mol cat/min)	16.0	16.0	4.7	4.4	3.7	65.1	20.0	58.0	29.3	26.4	44.6

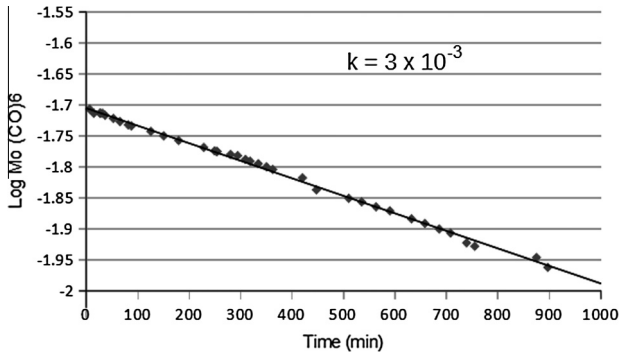

Fig. 1. A plot of sonolysis-assisted decomposition of $Mo(CO)_6$ in hexadecane in the presence of sulfur. The reaction conditions are noted in the experimental section.

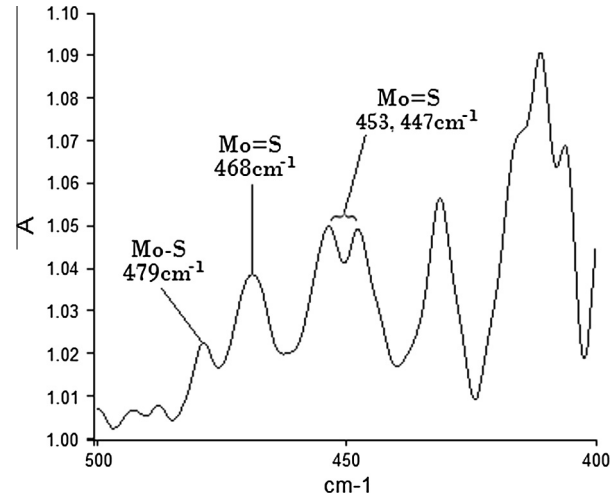

Fig. 2. FT-IR spectrum of black MoS_2 particles synthesized by sonication of $Mo(CO)_6$ and S_8 in hexadecane.

catalyst screening studies [60,61]. The reaction conditions and data are shown in Table 1 and the results are compared in Figs. 5–10. Note that the values in these figures are within 5%.

Figs. 5 and 6 show the effectiveness of the nano-MoS_2 catalyst for synthesis of higher alcohols, as measured by the total carbon conversion achieved during the run and the STY. With commercial micron-sized catalyst, the CO conversion maximized at 33%, irrespective of the solvent used: C-30 oil or PEG-400 both with and without the surfactant. Among all the runs with nano-sized MoS_2, the conversion maximized at 91.2% with a run in PEG-400 at 300 °C in the presence of 0.05 M Tergitol NP-8 surfactant (Fig. 5). Nano sizing a micron-sized (commercial) catalyst increases its surface area, a key parameter responsible for the observed increase in catalytic activity with nano-sized MoS_2 particles. However, the CO_2 production during HAS is wasted carbon, so a better measure of carbon conversion is CO_2-free basis or CO that leads to useful products, namely hydrocarbons or alcohols. The carbon conversion on a CO_2-free basis, a better picture emerges on carbon conversion. The CO conversion (on a CO_2-free basis) drops from 91.2% to 36.6% with the nano-MoS_2 and from 16.7 to 6.2 for the commercial catalyst (Fig. 5). The addition of surfactant to the commercial catalyst showed a decrease in CO conversion from 18.3% to 6.2%. However, the nano-sized MoS_2 catalyst showed an enhancement in the CO conversion from 21.1% to 28.6% with the addition of Tergitol NP-8 [0.01 M] in PEG-400 solvent. Overall, the results showed that the CO conversion is enhanced when the nano-sized MoS_2 is used in the presence of a surfactant (Fig. 6). The effect of temperature on carbon conversion was noted. At 300 °C, nano-MoS_2 in the presence of 50 mM surfactant produced higher CO_2 as by-product (compare Figs. 5 and 8). Without surfactant, the commercial catalyst (micron-sized MoS_2) achieved 32.0% CO conversion in C-30 oil solvent that dropped to 18.3% in PEG-400 solvent. Next, the production of C1–C4 hydrocarbons and STY of alcohols were compared for runs shown in Figs. 7 and 8. The nano MoS_2 catalyst runs, with and without surfactant, yielded an STY of 33.7 (mmol OH/mol cat./min) performing 39.7% higher than that of comparative commercial catalyst. On average, the surfactant enhanced nano-MoS_2 in a polar solvent had a higher STY of alcohols than in the absence of Tergitol NP-8 (3.67 mmol OH/mol cat/min). The observed increase in conversion and STY with the nano-sized MoS_2 are attributed to a higher surface area of the nanoparticles compared to the micron-sized particles of the commercial catalyst. The addition of a surfactant hindered carbon conversion of the commercial catalyst though it increased the conversion with the nano-sized MoS_2. This trend suggests that the particle sizes of the commercial catalysts is too large to be contained in the microemulsion droplet phase and may have increased aggregation of nanoparticles and destabilized the microemulsion phase. Whereas, smaller nano-sized MoS_2 particles are likely to be well dispersed in the hydrophobic droplet phase and thereby increase exposed surface area of the catalyst for HAS. The size seemed to affect selectivity to particular alcohol. The commercial catalyst showed selectivity toward C1–OH at 21.9% of total products without showing much difference with the addition of Tergitol NP-8. The nano-MoS_2 attained 33.3 mol% C2–OH selectivity (Fig. 9). The STY and selectivity of alcohols data were compared for runs at three Tergitol NP-8 concentrations of 2 mM, 11 mM and 53 mM in PEG-400 at 270 °C (Figs. 10 and 8). While at Tergitol concentration of up to 11 mM, no beneficial effect was seen, almost doubling of the STY was observed when the Tergitol NP-8 reached 53 mM (Fig. 8). On the other hand, the product selectivity still showed preference toward C2–OH (Fig. 10). However, the selectivity shifted toward C1–OH as the concentration of Tergitol NP-8

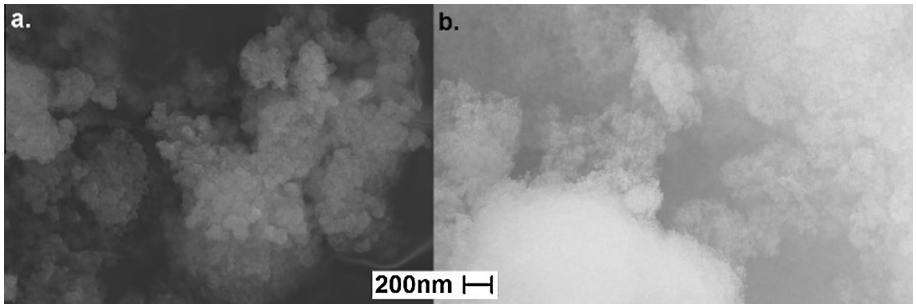

Fig. 3. SEM images of MoS_2 particles prepared by sonolysis (a) before the catalytic reaction; and (b) after the catalytic reaction with 0.01 M Tergitol NP-8 in PEG-400 (270 °C, 900 psi).

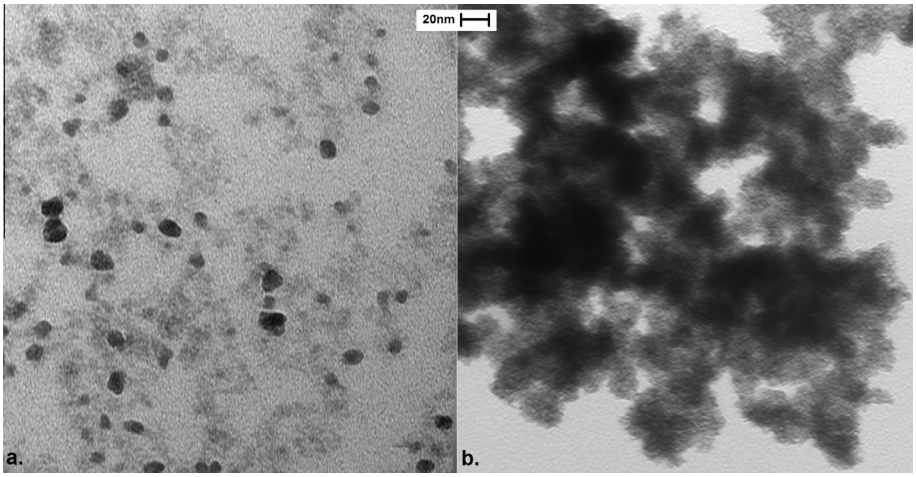

Fig. 4. TEM image of synthesized MoS_2 particles. (a) Freshly synthesized catalyst before the catalytic reaction; and (b) after the catalytic reaction with 0.01 M Tergitol NP-8 in PEG-400 (270 °C, 900 psi).

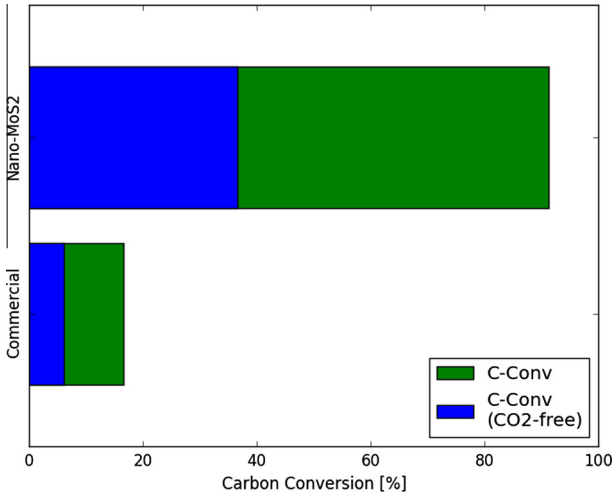

Fig. 5. Carbon conversion (blue) and CO_2-free basis carbon conversion (green) of syngas during HAS with commercial MoS_2 and nano-MoS_2 in PEG-400 solvent with Tergitol NP-8 (50 mM). T: 300 °C, P: 900 psi and Syngas: H_2/CO: 66%/34%. (For interpretation of the references to colour in this figure legend, the reader is referred to the web version of this article.)

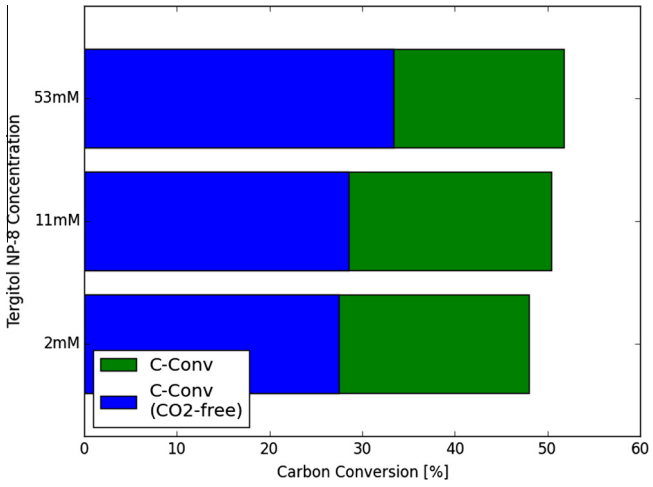

Fig. 6. Carbon conversion (blue) and CO_2-free basis carbon conversion (green) of syngas during HAS with nano-MoS_2 in PEG-400 solvent as a function of surfactant concentration. T: 270 °C, P: 900 psi. (For interpretation of the references to colour in this figure legend, the reader is referred to the web version of this article.)

increased (Fig. 10). Hydrocarbon analysis shows insignificant concentrations (<1%) of C5–C8 hydrocarbons.

4. Possible mechanisms for observed improvement in STY and selectivity

The hydrophobic phase consisting of syngas (sc-CO, sc-CO_2 and H_2), and nanoparticles are encapsulated in microemulsion droplets, thus increasing the interaction between the reactants and the catalyst particles (Fig. 11) while improving the mass and heat transfer rates. The mechanism proposed above would overcome limitations of the 4-phase system in which typical slurry systems for syngas catalysis operate by producing more homogeneous slurry for the reaction system. The use of supercritical medium as a solvent in heterogeneous multiphase catalytic systems is postulated to have several advantages: (1) increased gas–liquid mass transfer due to unlimited gas solubility in supercritical phase, (2) higher diffusion rates, (3) increased reaction rates due to higher solubility of products and (4) prevention of catalyst poisoning as well as improved reaction selectivity [10]. The F–T and alcohol synthesis reactions

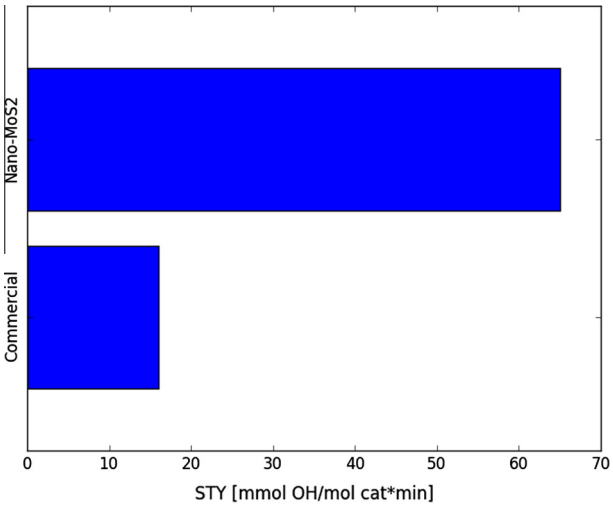

Fig. 7. STY (mmol OH/mol cat/min) of alcohols produced from syngas with commercial MoS_2 and nano-MoS_2 in PEG-400 solvent. P: 300 °C, P: 900 psi and syngas: H_2/CO: 66%/34%.

of syngas are generally not conducted in sc-CO_2 or sc-H_2O [11]. These solvents can alter the ratio of CO or H_2 through WGS or the reverse WGS reactions and this ratio critically determines the efficacy and selectivity of the F–T catalysts. Thus, supercritical hydrocarbon solvents such as methane, propane, pentane, and hexane have been investigated for F–T reactions [30–38] as well as for synthesis of methanol and higher alcohols from syn-gas [62–64]. An increase in conversion rates, improvement in mass and heat transfer rates and product selectivity was reported.

Even though we have not explicitly shown the formation of a microemulsion phase under the reaction conditions, we expect formation of such phase for the following reasons: CO_2 is known to form a microemulsion phase under supercritical conditions in water when stabilized by surfactants [65–69]. Similar data on CO and H_2 are lacking. However, the solubility of CO and H_2 in water are much lower than CO_2. The Bunsen coefficients of CO and H_2 at 298 K are 0.022 mL and 0.0176 mL per mL of pure water [70], respectively as compared to CO_2 (0.75–0.9 mL of CO_2 per mL of water) [71]. Thus, CO and H_2 molecules can be expected to form microemulsion phase in water or in similar hydrophilic phases when stabilized by surfactants. Additionally, the particles themselves can be used to stabilize the interface [72]. For example, oxides [73], carbon nanotubes [74], and hybrids of oxide–carbon nanotubes [75] as well as metal–carbon nanotubes [76] were used in stabilizing emulsion droplets. In particular, Pd-laden carbon nanotubes catalysts have been used to stabilize water–oil emulsions in a biomass-refining process application [33]. However, to our knowledge, there are no reports in literature in which microemulsion system have been used for syngas conversion to alcohols. Our work described here is the first that reports beneficial effects of microemulsion-based conversion of syngas to higher alcohols.

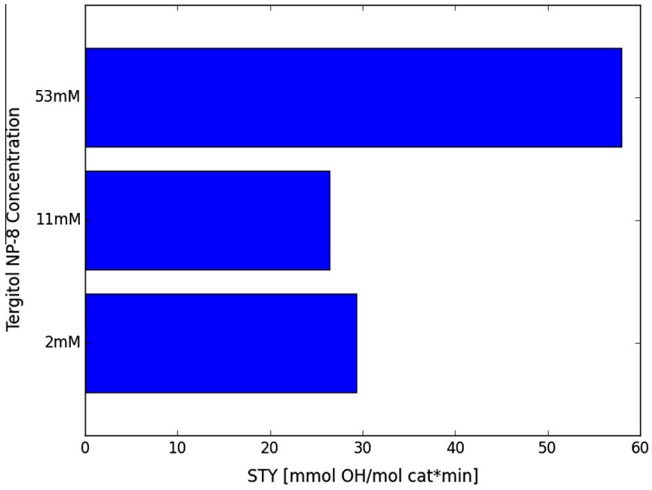

Fig. 8. STY (mmol OH/mol cat/min) of alcohols produced from syngas using nano-MoS_2 in PEG-400 solvent as a function of surfactant concentration. T: 270 °C, P: 800 psi and syngas: H_2/CO: 66%/34%.

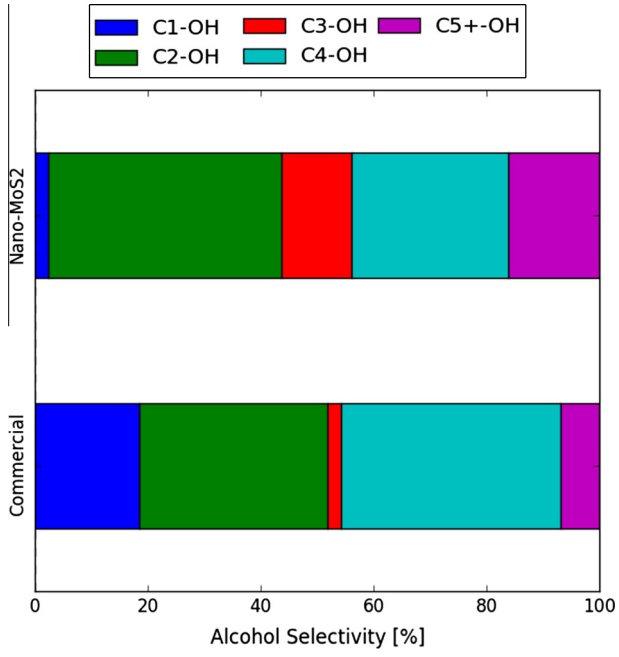

Fig. 9. Selectivity of alcohol products with commercial MoS_2 and nano-MoS_2 in PEG-400 solvent with Tergitol NP-8 (50 mM). T: 300 °C, P: 800 psi and syngas: H_2/CO: 66%/34%.

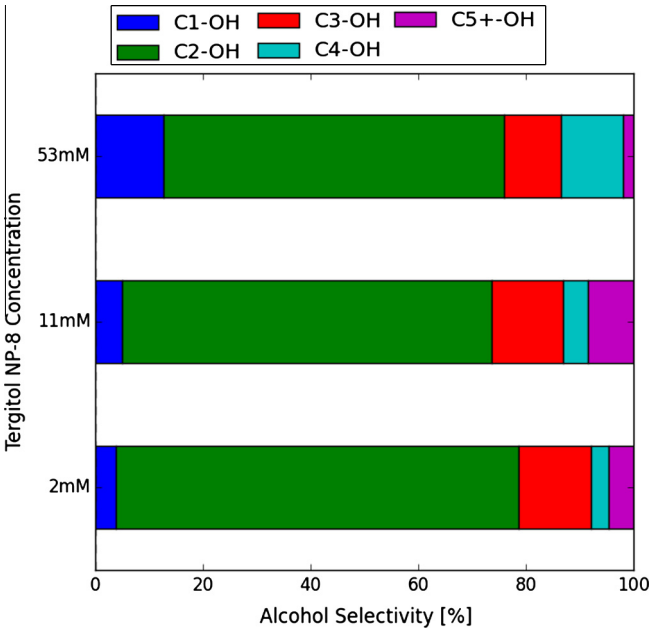

Fig. 10. Alcohol product selectivity in nano-MoS_2 catalyzed reaction in PEG-400 solvent as a function of surfactant concentration. T: 270 °C, P: 900 psi and syngas: H_2/CO: 66%/34%.

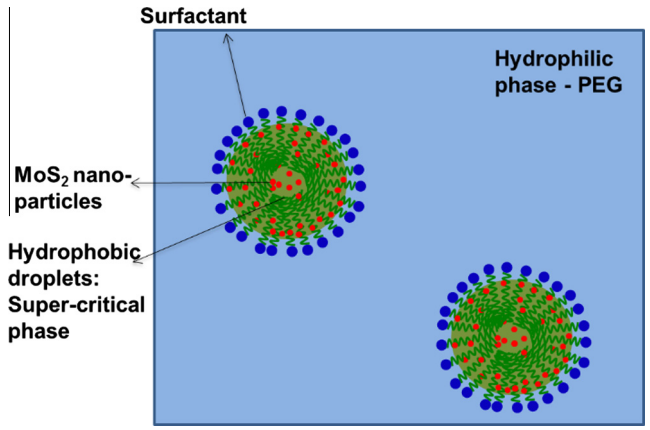

Fig. 11. Proposed mechanism for surfactant-enhanced catalytic reaction.

5. Conclusions

We have shown that nanoparticles of MoS_2 exhibit superior performance for HAS from syngas when carried out in a supercritical microemulsion medium. The microemulsions are stabilized by a non-ionic ethoxylated surfactant (Tergitol NP-8) in PEG-400 solvent as a continuous phase. A significant increase in STY for alcohol production as well as in selectivity for ethanol was observed with these encapsulated systems. A superior performance is attributed to a better dispersion of nanoparticles as well as improved mass and heat transfer characteristics of the system due to the use of microemulsion medium.

Funding sources

The project was funded through a supplemental Cooperative Opportunity between Industry/University Cooperative Research Centers (CORBI) grant from the National Science Foundation (NSF) at Stony Brook University, University of Hawaii and Columbia University sites.

Acknowledgements

The work was carried out at the NSF funded: Center for Bioenergy Research and Development (CBERD) at Stony Brook under NSF award number 0832520 and University of Hawaii sites as well as at the Center for Particular and Surfactant Systems (CPaSS) at Columbia University. Co-authors S.P. and P.S. acknowledge the funding support from NSF under award number 1336845.

References

[1] NOAA. Trends in atmospheric carbon dioxide. Earth System Research Laboratory; 2013. <http://www.esrl.noaa.gov>.
[2] EPA. Climate change: basic information; 2013. <www.epa.gov>.
[3] Billion-ton study. Oak Ridge National Lab. US Department of Energy; 2011.
[4] Grazaini M, Fornasiero P. In: Renewable resources and renewable energy: a global challenge. Taylor and Francis Group; 2007. p. 198–206.
[5] Air Products And Chemicals, Inc. IGCC process with combined methanol synthesis/water gas shift for methanol and electrical power production. Patent EP0336378 A2; 1989.
[6] Kang X et al. Advances in bifunctional catalysis for higher alcohol synthesis from syngas. Chin J Catal 2013;34:116–29.
[7] Spath P., Dayton D. Products from syngas-mixed higher alcohols (metal catalyst). Sun Grant Initiative & University of Tennessee; 2008. <http://bioweb.sungrant.org/Technical/Bioproducts/Bioproducts+from+Syngas/Mixed+Higher+Alcohols/Default.htm>.
[8] Andersson R et al. Correlation patterns and effect of syngas conversion level for product selectivity to alcohols and hydrocarbons over molybdenum sulfide based catalysts. Appl Catal A: Gen 2012;417–418:119–28.
[9] Herman RG. Classical and non-classical routes for alcohol synthesis [Chapter 7]. In: Guczi L, editor. New trends in CO activation. New York: Elsevier; 1991. p. 265–349.
[10] Kruse A, Vogel H. Heterogeneous catalysis in supercritical media: 1. Carbon dioxide. Chem Eng Technol 2008;31(1):23–32.
[11] Kruse A, Vogel H. Heterogeneous catalysis in supercritical media: Part 3. Other media. Chem Eng Technol 2008;31(10):1391–5.
[12] Kruse A, Vogel H. Heterogeneous catalysis in supercritical media: 2. Near-critical and supercritical water. Chem Eng Technol 2008;31(9):1241–5.
[13] King JW et al. Hydrogenation of vegetable oils using mixtures of supercritical carbon dioxide and hydrogen. J Am Oil Chem Soc 2001;78(2):107–13.
[14] Rovetto LJ et al. Supercritical hydrogenolysis of fatty acid methyl esters: phase equilibrium measurements on selected binary and ternary systems. J Supercrit Fluids 2005;35(3):182–96.
[15] Bertucco A et al. Catalytic hydrogenation in supercritical CO_2: kinetic measurements in a gradientless internal-recycle reactor. Ind Eng Chem Res 1997;36(7):2626–33.
[16] Zhao FY, Ikushima Y, Arai M. Hydrogenation of 2-butyne-1,4-diol to butane-1,4-diol in supercritical carbon dioxide. Green Chem 2003;5(5):656–8.
[17] Zhao FY, Ikushima Y, Arai M. Hydrogenation of 2-butyne-1,4-diol in supercritical carbon dioxide promoted by stainless steel reactor wall. Catal Today 2004;93(5):439–43.
[18] Jenzer G et al. Partial oxidation of alcohols in supercritical carbon dioxide. Chem Commun 2000(22):2247–8.
[19] Zhang RZ et al. Selective oxidation of cyclohexane in supercritical carbon dioxide over CoAPO-5 molecular sieves. Catal Today 2005;110(3-4):351–6.
[20] Sarsani VR, Wang Y, Subramaniam B. Toward stable solid acid catalysts for 1-butene plus isobutane alkylation: investigations of heteropolyacids in dense CO_2 media. Ind Eng Chem Res 2005;44(16):6491–5.
[21] Clark MC, Subramaniam B. 1-Hexene isomerization on a Pt/gamma-Al_2O_3 catalyst: the dramatic effects of feed peroxides on catalyst activity. Chem Eng Sci 1996;51(10):2369–77.
[22] Clark MC, Subramaniam B. Extended alkylate production activity during fixed-bed supercritical 1-butene/isobutane alkylation on solid acid catalysts using carbon dioxide as a diluent. Ind Eng Chem Res 1998;37(4):1243–50.
[23] Santana GM, Akgerman A. Alkylation of isobutane with 1-butene on a solid acid catalyst in supercritical reaction media. Ind Eng Chem Res 2001;40(18):3879–82.
[24] Marteel AE et al. Hydroformylation of 1-hexene in supercritical carbon dioxide: characterization, activity, and regioselectivity studies. Environ Sci Technol 2003;37(23):5424–31.
[25] Shibahara F, Nozaki K, Hiyama T. Solvent-free asymmetric olefin hydroformylation catalyzed by highly cross-linked polystyrene-supported (R, S)-BINAPHOS-Rh(I) complex. J Am Chem Soc 2003;125(28):8555–60.
[26] Tadd AR et al. Hydroformylation of 1-hexene in supercritical carbon dioxide using a heterogeneous rhodium catalyst. 1. Effect of process parameters. J Supercrit Fluids 2003;25(2):183–96.
[27] Hemminger O et al. Hydroformylation of 1-hexene in supercritical carbon dioxide using a heterogeneous rhodium catalyst. 3. Evaluation of solvent effects. Green Chem 2002;4(5):507–12.
[28] Jessop PG et al. Catalytic production of dimethyllformamide from supercritical cabon-dioxide. J Am Chem Soc 1994;116(19):8851–2.
[29] Jessop PG, Ikariya T, Noyori R. Homogeneous catalysis in supercritical fluids. Science 1995;269(5227):1065–9.
[30] Fan L, Fujimoto K. Fischer–Tropsch synthesis in supercritical fluid: characteristics and application. Appl Catal A: Gen 1999;186(1-2):343–54.
[31] Bukur DB et al. Effect of process conditions on olefin selectivity during conventional and supercritical Fischer–Tropsch synthesis. Ind Eng Chem Res 1997;36(7):2580–7.
[32] Lang XS, Akgerman A, Bukur DB. Steady-state Fischer–Tropsch synthesis in supercritical propane. Ind Eng Chem Res 1995;34(1):72–7.
[33] Fan L et al. Selective synthesis of wax from syngas by supercritical phase process: mass transfer effect of co-fed olefin. J Chem Eng Jpn 1997;30(3):557–62.
[34] Fan L, Yokota K, Fujimoto K. Supercritical phase Fischer–Tropsch synthesis – catalyst pore-size effect. AIChE J 1992;38(10):1639–48.
[35] Snavely K, Subramaniam B. On-line gas chromatographic analysis of Fischer–Tropsch synthesis products formed in a supercritical reaction medium. Ind Eng Chem Res 1997;36(10):4413–20.
[36] Yokota K, Fujimoto K. Supercritical phase Fischer–Tropsch synthesis reaction. Fuel 1989;68(2):255–6.
[37] Yokota K, Hanakata Y, Fujimoto K. Supercritical phase Fischer–Tropsch synthesis reaction: 3. Extraction capability of supercritical fluids. Fuel 1991;70(8):989–94.
[38] Jacobs G et al. Fischer–Tropsch synthesis: supercritical conversion using a Co/Al_2O_3 catalyst in a fixed bed reactor. Fuel 2003;82(10):1251–60.
[39] Herriott AW, Picker D. Phase transfer catalysis. Evaluation of catalysis. J Am Chem Soc 1975;97(9):2345–9.
[40] Starks CM. Phase-transfer catalysis. I. Heterogeneous reactions involving anion transfer by quaternary ammonium and phosphonium salts. J Am Chem Soc 1971;93(1):195–9.
[41] Makosza M. Phase-transfer catalysis. A general green methodology in organic synthesis. Pure Appl Chem 2000;72(7):1399–403.
[42] Tai Z, Zhang J, Wang A, Zheng M, Zhan T. Temperature-controlled phase-transfer catalysis for ethylene glycol production from cellulose. Chem Commun 2012;48:7052–4.
[43] Starks CM, Liotta CL, Halpern MC. Phase-transfer catalysis –fundamentals applications, and industrial, perspectives. New York: Springer; 1994. ISBN 0412040719.
[44] Park EJ, Kim MH, Kim DY. Enantioselective alkylation of b-keto esters by phase-transfer catalysis using chiral quaternary ammonium salts. J Org Chem 2004;69:6897.
[45] Lygo B, Andrews BI. Asymmetric phase-transfer catalysis utilizing chiral quaternary ammonium salts: asymmetric alkylation of glycine imines. Acc Chem Res 2004;37:518.
[46] Wladislaw B, Bueno MA, Marzorati L, DiVitta C, Zukerman-Schpector J. Phase transfer catalysis (PTC) sulfanylation of some 2-methylsulfinylcyclanones. J Org Chem 2004;69:9296.
[47] Lebel H, Morin S, Paquet V. Alkylation of phosphine boranes by phase-transfer catalysis. Org Lett 2003;5:2347.
[48] Barak G, Sasson Y. Effect of phase-transfer catalysis on the selectivity of hydrogen peroxide oxidation of aniline. J Org Chem 1989;54:3484.
[49] Zhang C, Zhang J, Li W, Feng X, Hou M, Han B. Formation of micelles of Pluronic block copolymers in PEG 200. J Colloid Interface Sci 2008;327:157–61.
[50] Ottinger I. Oral composition useful to treat conditions associated with renin activity (e.g. hypertension), comprising delta-amino-gamma-hydroxy-omega-aryl-alkanoic acid amide renin inhibitor in absorption enhancing medium. In: P.n. WO2005058291-A1, editor. NOVARTIS AG (NOVS-C) NOVARTIS PHARMA GMBH (NOVS-C); 2005.
[51] Cummings S, Enick R, Rogers S, Heenan R, Eastoe J. Amphiphiles for supercritical CO_2. Biochimie 2012;94:94–100.

[52] Xing D, Wei B, McLendon WJ, Enick RM, McNulty S, Trickett K, et al. CO_2-soluble, nonionic, water-soluble surfactants that stabilize CO_2-in-brine foams.
[53] Fang K, Li D, Lin M, Xiang M, Wei W, Sun Y. A short review of heterogeneous catalytic process for mixed alcohols synthesis via syngas. Catal Today 2009;147(2):133–8.
[54] Renewable fuels standard. EPA; 2013.
[55] Mahajan D, Papish ET, Pandya K. Sonolysis induced decomposition of metal carbonyls: kinetics and product characterization. Ultrason Sonochem 2004;11:385–92.
[56] Mahajan D, Marshall CL, Castagnola N, Hanson JC. Appl Catal A: Gen 2004;258:83–91.
[57] Nagaraju G et al. 2007;2(9):461–8.
[58] Parenago OP et al. Scientific problems of machines operation and maintenance 2010;1:161.
[59] Mahajan D, Vijayaraghavan P. Selective synthesis of mixed alcohols catalyzed by dissolved base-activated highly dispersed slurried iron. Fuel 1999;78 (1):93–100.
[60] Gerber MA, White JF, Stevens DJ. Mixed alcohol synthesis catalyst screening. Pacific Northwest National Laboratory; n.d. <Http://www.pnl.gov/main/publications/external/technical_reports/PNNL-16763.pdf>.
[61] Subramani V, Gangwal SK. A review of recent literature to search for an efficient catalytic process for the conversion of syngas to ethanol. Energy Fuels 2008;22(2):814–39.
[62] Liu JG, Qin ZF, Wang JG. Methanol synthesis under supercritical conditions: calculations of equilibrium conversions by using the Soave–Redlich–Kwong equation of state. Ind Eng Chem Res 2001;40(17):3801–5.
[63] Qin ZF, Liu JG, Wang JG. Solvent effects on higher alcohols synthesis under supercritical conditions: a thermodynamic consideration. Fuel Process Technol 2004;85(8-10):1175–92.
[64] Jiang T, Niu YQ, Zhong B. Synthesis of higher alcohols from syngas over Zn–Cr–K catalyst in supercritical fluids. Fuel Process Technol 2001;73(3):175–83.
[65] Eastoe J, Dupont A, Steytler DC, Thorpe M, Gurgel A, Heenan RKJ. Colloid Interf Sci 2003;258(2):367–73.
[66] Ihara T, Suzuki N, Maeda T, Sagara K, Hobo T. Chem Pharm Bull 1995;43:626.
[67] Lee CT, Ryoo W, Smith PG, Arellano J, Mitchell DR, Lagow RJ, Webber SE, Johnston KP. J Am Chem Soc 2003;125:3181.
[68] Schwan M, Kramer LGA, Sottmann T, Strey R. Phys Chem Chem Phys 2010;12:6247–52.
[69] Butler R, Hopkinson I, Cooper AI. J Am Chem Soc 2003;125(47):14473–81.
[70] Wiesenburg DA, Guinasso Jr NL. J Chem Eng Data 1979;24(4):356.
[71] Carroll JJ, Slupsky JD, Mather AE. J Phys Chem Data 1991;20(6):1201.
[72] Binks BP. Particles as surfactants—similarities and differences. Curr Opin Colloid Interface Sci 2002;7(1–2):21–41.
[73] Binks BP, Whitby CP. Silica particle-stabilized emulsions of silicone oil and water? Aspects of emulsification. Langmuir 2004;20(4):1130–7.
[74] Wang RK et al. Improving the effectiveness of interfacial trapping in removing single-walled carbon nanotube bundles. J Am Chem Soc 2008;130 (44):14721–8.
[75] Shen M, Resasco DE. Emulsions stabilized by carbon nanotube-silica nanohybrids. Langmuir 2009;25(18):10843–51.
[76] Crossley S et al. Solid nanoparticles that catalyze biofuel upgrade reactions at the water/oil interface. Science 2010;327(5961):68–72.